arXiv:physics/0201011v1 [physics.class-ph] 8 Jan 2002

Diamagnetic Interactions in Disordered Suspensions of Metastable Superconducting Granules

A. Peñaranda, C.E. Auguet and L. Ramírez-Piscina
Departament de Física Aplicada,
Universitat Politècnica de Catalunya,
Doctor Marañon 44, E-08028 Barcelona, SPAIN.
(February 2, 2008)

Abstract

The simulation of the transition sequence of superheated Type I superconducting granules (SSG) in disordered suspensions when an external magnetic field is slowly increased from zero has been studied. Simulation takes into account diamagnetic interactions and the presence of surface defects. Results have been obtained for the transition sequence and surface fields distribution covering a wide range of densities. These results are compared with previous analytical perturbative theory, which provides qualitative information on transitions and surface magnetic fields during transitions, but with a range of validity apparently limited to extremely dilute samples. Simulations taking into account the complete diamagnetic interactions between spheres appear to be a promising tool in interpreting SSG experiments, in applications such as particle detectors, and in some fundamental calculations of Solid State Physics.

KEYWORDS: A. Superconductors. A. Disordered systems. D. Phase transitions.

I. INTRODUCTION

The study of the electric and magnetic properties of inhomogeneous or disordered systems has been a subject of long-standing interest in both basic and applied condensed matter physics. Historically, studies of these properties have usually dealt with the determination of effective parameters (typically dielectric constants) on a longer spatial-scale than the typical scales of the inhomogeneities or the disorder[1]. However, in superconducting granular materials the situation is more complex and interesting. These systems, in response to applied fields, can suffer transitions which depend on details at the disorder scale. Moreover, as will become evident below, local fields change at every transition, which makes the response of the whole system history-dependent. In this context, mean or effective properties of these materials are of limited interest.

Measurements on superconducting granular materials can provide interesting information from a fundamental point of view. For example, the measurement of the supercritical fields of disordered suspensions of superconducting granules has yielded determinations of the Ginzburg-Landau parameters of the superconducting transition[2]. On the other hand, the superheated-to-normal phase transitions of Type I superconducting suspensions, induced by irradiation, have served as the basis for the recent development of particle detectors[3]; also the irradiation-induced supercooled normal-to-superconducting transition of granular arrays is being explored[4] with respect to dark matter detection in astroparticle physics.

In a superconducting granular material, the transition of each granule is determined by its position in its phase diagram, which is schematically shown in Fig. 1. Type I superconductors exhibit hysteresis, so a granule can traverse the equilibrium curve B_c without transiting as long as it remains in the metastable region. In Fig. 1 we show the case of an isolated metastable superconducting granule. It can be seen that the actual normal to superconducting transition, whether induced by a field increase ΔB or heating ΔT, depends critically on its location in the (T,B) phase space referred to the superheating field curve B_{sh}. Theoretically, this location is given by the bath temperature and the maximum field on the surface $B_{max} = (3/2)B_{ext}$. Experimentally, the location generally varies over a small range of fields as a result of surface and volume defects which act as nucleation centers[5,6]. In contrast, a disordered suspension exhibits a broader range of transition field values[7,8], which is generally due both to defects and to diamagnetic interactions between the superconductors themselves. This spreading depends directly on the local fields on the surface of the granules, information which is not directly accessible in experiments, and can reach typical values of 20%. Analogous behavior has been found in superconducting granule detectors, in which transitions occur by incident energy from particles or radiation. In this case the uncertainty in the minimum energy necessary for the transition necessarily hinders the interpretation of the results of these devices[7]. On the other hand, the long-range nature of the diamagnetic interaction produces changes in the surface field values for the entire system as each transition occurs. In consequence, the suspension disorder and its effects change with each transition. Therefore, it is clear that a complete theoretical analysis of diamagnetic interactions and their effects on transitions constitutes a first step in the interpretation of experiments involving this kind of suspensions.

There exist numerous theoretical results available on magnetic or (mathematically analogous) electric properties of disordered materials. These are mainly for the effective dielectric

constant of composites, involving mean field calculations, such as the classical mean-field Clausius-Mossotti or Maxwell-Garnett[9] approximation, rigorous bounds[10,11], or cluster expansions for suspensions of polarizable spheres[12,13]. Analogous expansions have been developed for the diamagnetic properties of superconducting sphere suspensions. In the regime of dilute suspensions, Geigenmüller[14] constructed a perturbative theory which is not limited to effective properties, but which calculates statistics of local surface fields on the granules and of the transitions induced by the external field. This theory is formally based on a cluster expansion in such a way that all the quantities are expanded in powers of the volume fraction ρ occupied by the microgranules. In practice, the expansion is performed up to first order, which means that only two-body interactions are considered[14]. Nevertheless, it provides the only analytical framework in which experiments have been interpreted so far.

In this paper we will study the magnetic properties of a disordered ensemble of (type I) superconducting granules immersed in an external magnetic field by numerical simulation. We specifically address the question of the diamagnetic interactions between granules, and the process of the successive transitions in the system induced by an increase of the external field. Relevant information, which is not experimentally accessible, such as local surface field values, is obtained during transitions. Conditions on which these transitions occur (essentially the external field values) are the crucial point in the applications mentioned above. The comparison of the simulation results to the perturbative calculation shows that the problem in interpreting experiments is twofold. Firstly, direct application of the perturbative results, which are valid in the dilute regime in principle, uses linear extrapolations of the experimental results to the zero-density limit as parameters of the theory. As we will show, the validity condition of this procedure (*i.e.* that experiments lie in the proper range of validity of the theory) is hardly fulfilled by current experimental results. Therefore, quantitative predictions are expected to fail in all density ranges. Secondly, some interesting results arise in measurements performed in high-density conditions, where diamagnetic interactions are most important and the perturbative theory does not apply. This is the case for instance of the experimental determination of the supercooling branch of the phase diagram and its associated Ginzburg-Landau parameters.[2] In each branch of a hystheresis loop, the last transiting granules are expected to be the most defect-free ones. Contrary to the superheating case, in a supercooling situation these granules are most affected by diamagnetic interaction of other superconducting granules. In view of all these circumstances, both the quantitative determination of the limits of validity of the perturbative calculation, and the use of simulation to obtain results valid in the whole density regime are of prime interest.

The structure of this paper is the following. The simulation procedure is described in detail in Section II. Results obtained for representative cases, presented in Section III, show the critical importance of diamagnetic interactions in the transitions of disordered superconducting suspensions, and quantitatively demonstrate the limited range of validity of the perturbation theory. In Section IV some conclusions are drawn from this work.

II. SIMULATION DETAILS

We performed simulations of dispersions of N superconducting spheres of radius a sited in positions given by $\mathbf{R}_i$ in a thin cylindrical sample of thickness L and radius $\alpha \times L$.

Positions were chosen at random in the prescribed volume excluding configurations in which the distance between the centers of any couple of spheres is $d \leq 2a$. An external field B_{ext} applied to the system was considered. The radius of the spheres was considered much greater than the London penetration length, and the transitions of each sphere to the normal phase are completed when the local magnetic field on any point of its surface reaches a threshold value B_{th}. Hence, we do not consider partial transitions to the intermediate state. This is justified when the local magnetic field applied over a sphere is greater than the critical magnetic field B_c, and thus the sphere is in a metastable state[14]. Neither the possible effects of diamagnetic contact and associated percolation phenomena for very concentrated configurations were considered. The magnetic field $\mathbf{B}(\mathbf{r})$ can be determined from a scalar potential $U(\mathbf{r})$

$$\mathbf{B}(\mathbf{r}) = -\nabla U(\mathbf{r}), \tag{1}$$

which satisfies the Laplace equation

$$\nabla^2 U(\mathbf{r}) = 0. \tag{2}$$

with the following boundary conditions. Firstly, for any superconducting sphere the magnetic field is tangential to the surface, *i.e.* the normal derivative of the potential vanishes there. Secondly, the value of the field very far from the sample should match $\mathbf{B}_{ext}$:

$$U(\mathbf{r}) \to -\mathbf{r} \cdot \mathbf{B}_{ext} \;\; (r \to \infty). \tag{3}$$

The scalar potential $U(\mathbf{R}_j + \mathbf{r}_j)$ near sphere j can be expanded in multipoles[14,15] which, introducing the boundary conditions at the surface of the sphere, can be written as

$$U(\mathbf{R}_j + \mathbf{r}_j) = \sum_{\lambda=1}^{\infty} \sum_{\mu=-\lambda}^{\lambda} Y_{\lambda\mu}(\hat{r}_j)\; c_{\lambda\mu}(j) \left\{ \left(\frac{a}{r_j}\right)^{\lambda+1} + \frac{\lambda+1}{\lambda} \left(\frac{r_j}{a}\right)^{\lambda} \right\} + K(j), \tag{4}$$

where $Y_{\lambda\mu}(\hat{r}_j)$ are spherical harmonics, and $c_{\lambda\mu}(j)$ and $K(j)$ are the coefficients of the expansion. There is one of these expansions for each sphere.

From all the expansions, and employing the boundary conditions, the coefficients satisfy the following equations[15]:

$$K(j) = -\mathbf{R}_j \cdot \mathbf{B}_{ext} + \sum_{k \neq j} \sum_{\lambda=1}^{\infty} \sum_{\mu=-\lambda}^{\lambda} A_{00\,\lambda\mu}(j,k)\; c_{\lambda\mu}(k) \tag{5}$$

$$\frac{\lambda+1}{\lambda}\; c_{\lambda\mu}(j) = -\sqrt{\frac{4\pi}{3}} B_{ext}\; a\; \delta_{\lambda 1}\delta_{\mu 0} + \sum_{k \neq j} \sum_{\lambda'=1}^{\infty} \sum_{\mu'=-\lambda'}^{\lambda'} A_{\lambda\mu\,\lambda'\mu'}(j,k)\; c_{\lambda'\mu'}(k) \tag{6}$$

where the constants $A_{\lambda\mu\,\lambda'\mu'}(j,k)$ are given in Ref.[16]. Without loss of generality, in Eq. (6) we have placed the external field in the z-direction. After determining the values of the unknowns $c_{\lambda\mu}(j)$ and $K(j)$ for a given configuration, it is possible to calculate the surface fields from Eq. (4).

The constants $K(j)$ only give additive contributions to the potential and do not affect the magnetic field values, so the problem is, in principle, to solve the infinite set of linear equations (6) for the unknown c's. In practice one only takes into account a limited number of multipolar terms according to the desired precision. Even then, the number of unknowns is so large that a direct solution of the Eqs. (6) is a formidable task for configurations with a representative number N of spheres. Instead, we employ the following iterative method[16]. Eq. (6) can formally be written as a matrix equation for the vector of unknown $\mathbf{c}$

$$\mathbf{c} = \mathbf{b} + A\mathbf{c} \tag{7}$$

whose solution is

$$\mathbf{c} = (I - A)^{-1}\mathbf{b} \tag{8}$$

which can be expanded as a power series in A,

$$\mathbf{c} = \left(I + A + A^2 + A^3 + ...\right)\mathbf{b}. \tag{9}$$

The simplest way to numerically perform this expansion is to apply the iteration

$$\mathbf{c}_{i+1} = \mathbf{b} + A\mathbf{c}_i, \tag{10}$$

$$\mathbf{c}_0 = \mathbf{b}. \tag{11}$$

The dependence of the A matrix elements on the distance between the spheres guarantees the convergence of this expansion, which is faster for more dilute systems. The desired precision is achieved by iteratively applying Eq. (10) until the change of the coefficients c is lower than a prescribed value.

The procedure in our simulations is then as follows: N superconducting spheres are placed at random in the desired geometry according to the value of the given filling factor ρ (fraction of volume occupied by the microgranules). The threshold values B_{th} for every sphere are also assigned by using a given distribution. Applying the iterative method described above, the values of the coefficients c are obtained, which enables determination of the local values of the magnetic field on the surface of any sphere from Eqs. (1,4). The maximum value of the surface field for each sphere is then calculated by standard routines of minimization of multivariate functions. The comparison of these maximum surface fields with the respective values of B_{th} permits selection of the first superconducting sphere that will transit to normal under an increase of the applied magnetic field. Furthermore, the precise value of B_{ext} at which the transition occurs is monitored. Subsequently, the system becomes one of $N - 1$ superconducting spheres. The long-range nature of the diamagnetic interactions changes the surface magnetic field values of the remaining superconducting spheres on any transition. This leads us to repeat the same calculation process after each transition until all spheres have transited.

III. RESULTS AND DISCUSSION

For the simulations we have employed a distribution of values of B_{th} consistent with experimental results for tin microspheres diluted in paraffin[17]. A parabolic distribution fit is

used in the interval between $0.8B_{sh}$ and B_{sh}[14,15]. This distribution of B_{th} values was obtained from experimental data corresponding to systems with small ρ extrapolated to $\rho = 0$. The number of initially superconducting spheres employed in simulations was $N = 250$ for dilute dispersions with ρ values from 0.001 up to 0.05, and $N = 150$ for denser systems with ρ up to 0.20. For each case we performed averages over a number of independent configurations between 2 to 7. The geometrical ratio α was chosen to be 10. This large value of α makes finite-size effects important for the larger volume fractions employed. Indeed for $\rho = 0.20$ a system of $N = 150$ has a width of only 4.6 sphere radius, and hence cannot be considered as truly 3- dimensional. However, it also avoids the appearance at these densities of percolating clusters associated to diamagnetic contact, which in fact has been ignored in simulations.

The fraction f of remaining superconducting spheres during an increase of the external field is shown in Fig. 2 versus B_{ext} for different values of ρ. The furthest to the right continuous line in this figure shows the expected behavior for isolated spheres, for which the maximum surface field is equal to $3/2B_{ext}$, and therefore can be directly related to the distribution of B_{th} values. We see that for the most dilute case ($\rho = 0.001$) the f values closely follow that $\rho = 0$ limit, except for a few transitions occurring earlier than expected corresponding to spheres whose distances to the nearest neighbor are not very large (about $0.10 - 0.15$ times the radius value). Therefore, for such a dilute case, the observed spread in the transition field values can be attributed to surface defects. However, Fig. 2 shows transitions for increasingly lower external fields as the concentrations of the sample are increased. This enhanced spread in the transition fields is produced by the diamagnetic interactions between spheres in these more densely packed configurations, which generate local surface fields much higher than the externally applied field and are the origin of the observed dependence on the sample filling factor. We see that diamagnetic interactions start to be the most important factor in transition spreading for filling factors of a few per cent. Indeed half of the spheres have undergone transitions at $B_{ext} = 0.48B_{sh}$ for $\rho = 0.20$, while for $\rho = 0.001$ a field $B_{ext} = 0.60B_{sh}$ is required. Similar behavior was observed in the experimental results of Dubos and Larrea[18]. In these experiments half of the spheres transited at $B_{ext} = 0.48B_{sh}$ for $\rho = 0.25$, at $B_{ext} = 0.50B_{sh}$ for $\rho = 0.20$, and $B_{ext} = 0.53B_{sh}$ for $\rho = 0.04$. This agreement confirms that the mechanisms implemented in the simulations (presence of surface defects and influence of diamagnetic interactions) are essentially correct.

These results suggest an analysis of our results in terms of the perturbative theory of Geigenmüller[14], which takes into account these mechanisms under the same hypotheses (ignoring partial transitions, diamagnetic contact, etc) assumed in our numerical simulations. This theory performs a systematic expansion of quantities such as the surface field distribution and the transition sequence in powers of the filling factor. Within the framework of this expansion we can write[14]:

$$f(B_{ext}, \rho) = f_0(B_{ext}) + \rho f_1(B_{ext}) + O(\rho^2) \tag{12}$$

where the zeroth order is the same $\rho = 0$ prediction represented in Fig. 2. This expansion shows how the distribution of B_{th} can be obtained from experimental data by performing measurements on samples of different densities and extrapolating the results to $\rho \to 0$[14,15,17]. In this expansion, each order can be calculated from this distribution of threshold fields B_{th}, and involves increasingly higher order contributions both in the number of spheres and in multipolar interactions. In the present state of the theory, calculations are done up to first

order, which is equivalent to considering only two-body interactions.

The comparison between our simulations and the results of the Geigenmüller theory should permit one to define the range of validity of the linear approximation, and provide an insight into the effects of higher order terms. To this end Fig. 2 also shows the predictions of Eq. 12 and Ref.[14] for $\rho = 0$, 0.01, 0.05 and 0.10 as continuous lines. We see that the theory does contain the observed trend of transitions to occur for lower external fields due to diamagnetic interactions, but agreement does not seem to be quantitative except for extremely dilute samples. For the 5% case agreement appears to be rather poor and it is worse for denser systems.

A more appropriate test of the linear approximation involved in Eq. 12 is the study of the dependence of f on the density ρ for different values of B_{ext}. This is shown in Fig. 3, where symbols represent simulation results and lines are the perturbative predictions of Eq. 12. Note that the evolution of a system during successive transitions is represented by points at constant ρ and increasing values of B_{ext}. We see that the perturbative calculation of Eq. 12 provides a correct qualitative picture of the transitions. However, for intermediate values of B_{ext}, the differences between theory and simulations begin to be non-negligible at volume fractions between 2 - 5%. These results further indicate that $\rho \to 0$ extrapolations of experimental results, performed in order to obtain information on the distribution of values of B_{th}, should only be made with very dilute systems. This may explain the apparent discrepancies between theory and experiment found in Refs.[14,17], where the values of f_0 and f_1 were evaluated by linear extrapolations of experimental data up to $\rho = 5\%$. In view of Fig. 3, this procedure should yield erroneous results in the range of the most interesting values of B_{ext}, where transitions mostly occur. It is precisely in this range where the contribution of f_1 in Eq. 12 is more important, so it is here where a breakdown of the perturbative scheme is expected[14]. We will address this point below.

The study of the maximum values of the magnetic field on the surface of the granules is the key point in analyzing the transitions, as pointed out above. This is a quantity that is not accessible to direct experimental measurements. The theory of Geigenmüller provides estimates of the distribution of values of such maximum fields in the small-density expansion[14]:

$$P(B_{max}, \rho) = P_0(B_{max}) + \rho P_1(B_{max}) + O(\rho^2) \tag{13}$$

In this equation $P(B_{max}, \rho)$ stands for the fraction of superconducting spheres with a maximum surface magnetic field smaller than B_{max}. We have omitted the implicit dependence of such quantities on B_{ext}. $P_0(B_{max})$ is the step function $\theta(B_{max} - 3/2B_{ext})$, *i.e.* the result for isolated spheres. The linear term describes the broadening of the distribution due to magnetic interactions[14]. These interactions change at each transition during the increase of the external field, and therefore are history dependent. This is the reason why the broadening described by P_1 depends on B_{ext}.

The problem of a systematic expansion in ρ of quantities such as the distribution $P(B_{max}, \rho)$ is that by its own nature the zeroth order is discontinuous, while the effect of a finite ρ should smooth it. However, it is impossible that a linear correction such as Eq. 13 could do this job for all values of ρ. In fact, looking closely at the prediction of Eq. 13 around $B_{max} = 3/2B_{ext}$ we can check that there exists a discontinuity and the distribution function ceases to be monotonous. This breakdown of the perturbative theory is shown in

Fig. 4, where we represent the predictions of the theory for a dilute case ($\rho = 0.01$) and a concentrated case ($\rho = 0.20$) at an applied external field $B_{ext} = 0.5B_{sh}$. At this value of B_{ext} all transitions are exclusively due to diamagnetic interactions, and whereas for dilute systems only a small fraction have occurred, for more concentrated configurations the system is deeply immersed in the transition sequence. We see that two branches appear on both sides of the discontinuity at $B_{max} = 3/2B_{ext}$. While both branches are close to each other for small ρ and one could use some criterion to connect them, for large ρ this is not the case. We have chosen to use the right-hand side branch in such situations to extract quantitative information and to compare it with simulations.

In Fig. 5 we show simulation and perturbative results of the distribution P of maximum surface fields for systems at $B_{ext} = 0.2B_{sh}$ and different initial values of ρ. These results are almost identical to the results without transitions of Ref.[16]. For this value of the external field, only a reduced number of spheres have already transited, and what one sees is the result of the diamagnetic interactions on almost completely disordered configurations of superconducting spheres. Again, although the perturbative theory qualitatively describes the diamagnetic effects, namely the broadening of the maximum field distribution, it only appears as quantitatively correct for very small values of the occupied volume fraction. In Fig. 6 we show the analogous results for an external field $B_{ext} = 0.6B_{sh}$. For this field the system has already suffered a large number of transitions except for the extremely dilute configurations. Here the convergence of the perturbative expansion is expected to be rather limited, and, in fact, its non-analytical behavior at $B_{max} = 3/2B_{ext}$ is clearly seen. However the perturbative theory (the right-hand side branch) continues to provide satisfactory qualitative predictions. Note that the maximum field distributions are much narrower after this increase of the external field. In fact, when a large number of spheres have transited induced by the external field, those that remain superconducting are expected to form quite ordered configurations[19,20], and, as a consequence, the surface field values become more uniform in the sample[19]. This feature is captured by the perturbative theory.

In order to show the ordering effect of the transitions more clearly we present the evolution of the distribution P during the increase of B_{ext} for three systems with representative values of the filling factor: $\rho = 0.001$ (Fig. 7), $\rho = 0.01$ (Fig. 8) and $\rho = 0.20$ (Fig. 9). For each filling factor, both simulations and perturbative results are shown for values of the external field ranging from $0.2B_{sh}$ up to $0.6B_{sh}$, for which most transitions occur. We see again that the broadening of the field distribution is drastically reduced as the external field is increased. The results indicate discrepancies between the perturbative theory and the simulations for the lowest values of B_{ext} even for very dilute systems. However, agreement improves as B_{ext} increases and the systems undergo transitions.

The results obtained for the most dense system with a volume fraction $\rho = 0.20$ (Fig. 9) are particularly interesting: the large discrepancies observed at $B_{ext} = 0.2B_{sh}$ evolve to a fair agreement for $B_{ext} = 0.5B_{sh}$ or $B_{ext} = 0.6B_{sh}$. In Fig. 10 we characterize the distribution of maximum surface fields for this filling factor by its mean and its standard deviation values, which are represented versus the increasing external field and compared with the perturbative theory. One feature of the theory that is visible here is that it predicts transitions only for external fields greater than $0.2B_{sh}$. We see that the surface fields approach the isolated sphere values as B_{ext} increases, whereas the standard deviation approaches zero indicating an increase of the uniformity of the system. We also see that the theory approaches the

simulation results quite satisfactorily for external fields greater than $0.4B_{sh}$.

This agreement after transitions between simulations and a small density approximation is quite surprising for such a dense case, and appears to be better than that obtained for low densities and low external field. One possible explanation could be that when a large number of transitions have occurred, the effective filling factor (if we only take into account the remaining superconducting spheres) is smaller, and one could expect a better convergence of the ρ-expansion. However, this agreement corresponds to systems with effective volume fractions after transitions that are higher than in the low field systems represented in Figs. 7 and 8 for $\rho = 0.001$ and 0.01. This can be seen in Fig. 11, where we have represented the mean and standard deviation of the maximum surface fields versus the effective filling factor ρ_{ef} for the dense system with initial $\rho = 0.20$. In this figure the evolution of the system is to decreasing values of ρ_{ef}. We already see good agreement for $\rho_{ef} = 0.1$, which is a rather large value. To show this, in Fig. 9 we have also represented the distribution of maximum fields for a configuration with the same ρ_{ef} (slightly lower than 0.1) than that of $B_{ext} = 0.5B_{sh}$, but with positions completely at random, and the corresponding predictions from perturbative theory. Note the good agreement between theory and simulations for the system which has been ordered by transitions compared with the discrepancies observed for the last random configuration with the same effective filling factor. We can conclude that the perturbative theory implicitly includes the observed tendency to form ordered configurations of remaining superconducting spheres, and that it describes these resulting configurations quite well, even if they arise from much more concentrated initial systems. However this good behavior of the theory is not completely explained by the decrease of the effective filling factor during the transition process.

IV. SUMMARY AND CONCLUSIONS

In summary, we have performed numerical simulations of disordered suspensions of superheated superconducting granules (SSG), transiting to normal when an external magnetic field is slowly increased from zero. Transitions are controlled by the local surface magnetic fields, which depend in a non-trivial way on the geometrical configuration of the superconducting granules via strong diamagnetic interactions, and the presence of surface defects. Performed simulations employ complete resolutions of the Laplace equation for the magnetic field with suitable boundary conditions on the surface of the superconducting spheres, and therefore are expected to provide results which are not limited to dilute samples. Consistent comparison with previous experimental results indicates that the simulations capture the mechanisms involved in the real system, and their use in simulations appears to be essentially correct. A better comparison with experimental results might need a revision of the B_{th} distribution. Also the employ of a larger number of spheres in simulations could be necessary to reduce finite-size effects[16]. On the other hand, the numerical method can be straightforwardly generalized to SSG configurations with spheres of different sizes. Preliminary simulations with realistic size distributions show the same qualitative behaviour than obtained with spheres of equal radius.

Transition sequences as a function of the (increasing) applied field have been obtained for a large range of granule concentrations. Distributions of local maximum surface fields, a relevant quantity in interpreting SSG experiments but not directly measurable, have also

been obtained. Results indicate a non-negligible effect of diamagnetic interactions between spheres, even for dilute systems, manifested in transitions occurring for lower external fields. These interactions appear as the most dominant factor in transitions for filling factors starting at a few per cent. The distribution of maximum surface fields becomes wider for denser configurations owing to diamagnetic interactions, but successive transitions induced for these interactions reduce the dispersion of these surface fields. This homogenising effect is associated with a positional ordering of the remaining superconducting spheres, and should be an important factor in reducing the energy uncertainty in detection applications of SSG systems.

We have compared simulation results of both transitions and surface field distributions with the analytical cluster expansion of Geigenmüller[14]. Theory and simulations share the same mechanisms (diamagnetic interactions and surface defects), and the same hypothesis (not considering partial transitions nor diamagnetic contacts) in modeling SSG systems. However the theory has been developed up to first order in the filling factor, which limits the calculation to two body interactions. Simulation results show that the perturbative theory qualitatively predicts the behavior of the system, namely the dependence of the transitions and the maximum surface fields on the concentration of the sample and on the value of the external applied field. However, perturbative theory is quantitatively correct only for very dilute samples, with occupied volume fractions of at most 1 - 2%. This range of validity increases for systems initially at higher densities after having undergone a large number of transitions. The ordering of these resulting configurations is well described by the theory.

As a final conclusion, diamagnetic interactions appear to be a factor of fundamental concern in SSG systems. Results from perturbative expansions, although providing a very useful framework for analyzing experiments, have a rather limited range of validity, and should be used with caution in obtaining quantitative information. In particular, extrapolation to the zero concentration limit of experimental data should only be performed for very dilute samples, within the validity range of the expansion. The use of simulations to obtain results for all densities should become an essential tool in interpreting SSG experiments. In this sense, generalization of the theoretical framework in which both simulations and perturbative theory are based could be essential to analyze very concentrated systems, in which partial transitions due to diamagnetic contact can occur.

These results, or more properly the numerical techniques in obtaining them, may also be of interest in a re-examination of the earlier Ginzburg-Landau parameter determinations from multi-grain measurements of the supercooled-to-superconducting transition. This numerical approach should also be of use in areas of condensed matter physics other than superconductivity, such as viscous fluid flow through a disordered porous medium, where similar equations arise, or investigation of the magnetic properties of ultrathin ferromagnetic films[21].

ACKNOWLEDGMENTS

We would like to thank T. Girard for helpful discussions and manuscript corrections. We acknowledge financial support from Dirección General de Investigación Científica y Técnica (Spain) (Projects BFM2000-0624-C03-02 and PB98-1203), Comissionat per a Universitats

i Recerca (Spain) (Projects 1999SGR00145 and 2000XT-0005), and European Commision (Project TMR-ERBFMRXCT96-0085). We also acknowledge computing support from Fundació Catalana per a la Recerca-Centre de Supercomputació de Catalunya (Spain).

REFERENCES

[1] *Electrical transport and optical properties of inhomogeneous media*, Ed. J.C. Garland and D.B. Tanner, AIP Conf. Proc. No. **40** (AIP, New York, 1978), and references therein.

[2] F.W. Smith, A. Baratoff and M. Cardona, Phys. Kondens. Materie **12**, 145 (1970); A. Larrea, A. Morales, G. Waysand and J. Bartolome, Nucl. Inst. and Meth. **A317** 541 (1992).

[3] *Superconductivity and Particle Detection*, ed. TA Girard, A. Morales and G. Waysand (World Scientific, Singapore, 1995), and references within.

[4] G. Meagher, D. DiSanto, A. Kotlicki, G. Eska and B.G. Turrell, Phys. Rev. Lett. **79**, 285 (1997).

[5] J. Feder and D. McLachlin, Phys. Rev. **177**, 763 (1969).

[6] D. Hueber, C. Valette and G. Waysand, J. Physique Lettres **41**, 4611(1980); D. Hueber, C. Valette and G. Waysand, Physica **108B**, 1229 (1981).

[7] A.K. Drukier and C. Vallete, Nucl. Instrum. Methods, **105**, 285 (1972); A.K. Drukier, Nucl. Instrum. Methods, **173**, 259 (1980), ibid **201**, 77 (1982).

[8] M. Furlan and K. Schmiemann, Nucl. Instrum. Methods, A **374**, 413 (1996).

[9] J.C.M. Garnett, Phil. T. Roy. Soc. A **203**, 385 (1904).

[10] D.J. Bergman, Phys. Rep. **43**, 377 (1978).

[11] G.W. Milton, R.C. McPhedran and D.R. McKenzie, Appl. Phys. **25**, 23 (1981)

[12] U. Geigenmüller, Physica **136 A**, 316 (1986).

[13] B.U. Felderhof, G.W. Ford and E.G.D. Cohen, J. Stat. Phys. **28**, 135 (1982), and J. Stat. Phys. **28**, 649 (1982).

[14] U. Geigenmüller, J. Phys. France **49**, 405 (1988).

[15] U. Geigenmüller, in *Superconducting and Low-Temperature Particle Detectors*, ed. G. Waysand and G. Chardin (Elsevier, Amsterdam, 1989).

[16] A. Peñaranda, C.E. Auguet and L. Ramírez-Piscina, Nucl. Instrum. and Meth. **A424**, 512 (1999).

[17] B. Mettout, Thesis, Université Paris VII, June 1988.

[18] H. Dubos et al, Phys. Rev. **B58**, 6468 (1998); A. Larrea et al, Nucl. Instrum. and Meth. **A317**, 541 (1992).

[19] A. Peñaranda, C.E. Auguet and L. Ramírez-Piscina, Sol. State Comm. **109**, 277 (1999).

[20] C. Valette, G. Waysand and D. Stauffer, Solid State Commun. **41**, 305 (1982); M. Hiller and D. Stauffer, Sol. State Comm. **43**, 487 (1982).

[21] L. Hu, H. Li and R. Tao, Phys. Rev. **B60**, 10222 (1999-II).

FIGURES

FIG. 1. Phase diagram for a type I superconductor. ΔB and ΔT represent the increase of either the magnetic field or the temperature needed for a transition to the normal state.

FIG. 2. Fraction f of spheres that remain superconducting versus B_{ext}/B_{sh}, after an increase of the external magnetic field from zero, for different occupied volume fractions ρ. Symbols represent simulation results. From right to left, continuous lines correspond to predictions of Eq. 12 and Ref.[14] for $\rho = 0$, 0.01, 0.05 and 0.10. The case of $\rho = 0$ is the dilute limit, *i.e.* assuming a maximum surface field of $1.5B_{ext}$ for all the spheres.

FIG. 3. Fraction f of spheres that remain superconducting in function of ρ for several values of the increasing B_{ext}. Symbols are simulation results: ($\circ$) $B_{ext} = 0.30B_{sh}$, ($\times$) $B_{ext} = 0.40B_{sh}$, squares $B_{ext} = 0.50B_{sh}$, ($*$) $B_{ext} = 0.53B_{sh}$, ($\diamond$) $B_{ext} = 0.55B_{sh}$, ($+$) $B_{ext} = 0.58B_{sh}$, ($\triangle$) $B_{ext} = 0.60B_{sh}$, ($\bullet$) $B_{ext} = 0.62B_{sh}$, full squares $B_{ext} = 0.65B_{sh}$. From the top to the bottom, continuous lines are predictions of Eq. 12 and Ref.[14] for the same values of B_{ext}.

FIG. 4. Fraction P of spheres with maximum surface field lower than the x-axis value (in units of B_{ext}), obtained from Eq. 13 and Ref.[14], when the external magnetic field has reached the value $0.5B_{sh}$, for $\rho = 0.01$ and $\rho = 0.20$. The right branch was chosen to extract quantitative information.

FIG. 5. Fraction P of spheres with maximum surface field lower than the x-axis value (in units of B_{ext}), when the external magnetic field has reached the value $0.2B_{sh}$, for several values of ρ. Continuous lines are the corresponding predictions of Eq. 13 and Ref.[14]

FIG. 6. Fraction P of spheres with maximum surface field lower than the x-axis value (in units of B_{ext}), when the external magnetic field has reached the value $0.6B_{sh}$, for several values of ρ. Continuous lines are the corresponding predictions of Eq. 13 and Ref.[14]

FIG. 7. Fraction P of spheres with maximum surface field lower than the x-axis value (in units of B_{ext}), corresponding to an initial $\rho = 0.001$ for several values of external magnetic field Continuous lines are the corresponding predictions of Eq. 13 and Ref.[14]

FIG. 8. Fraction P of spheres with maximum surface field lower than the x-axis value (in units of B_{ext}), corresponding to an initial $\rho = 0.01$ for several values of external magnetic field Continuous lines are the corresponding predictions of Eq. 13 and Ref.[14]

FIG. 9. Fraction P of spheres with maximum surface field lower than the x-axis value (in units of B_{ext}), corresponding to an initial $\rho = 0.20$ for several values of external magnetic field. The results for a system with the same number of spheres that remain superconconducting in the case of $B_{ext} = 0.5B_{sh}$ but placed at random are also represented. Continuous lines are the corresponding predictions of Eq. 13 and Ref.[14] Dashed line corresponds to the prediction for the random configuration.

FIG. 10. Mean and standard deviation values(in units of B_{ext}) corresponding to the distribution of maximum surface fields versus the increasing external field for initial $\rho = 0.20$. The results from the simulations and from the perturbative theory (GT) are represented.

FIG. 11. Mean and standard deviation values(in units of B_{ext}) corresponding to the distribution of maximum surface fields versus the resulting effective filling factor ρ_{ef}. The results from the simulations and from the perturbative theory (GT) are represented for a system with initial $\rho = 0.20$ through progressive increasing of the external field.

Fig. 1 Penaranda et al.

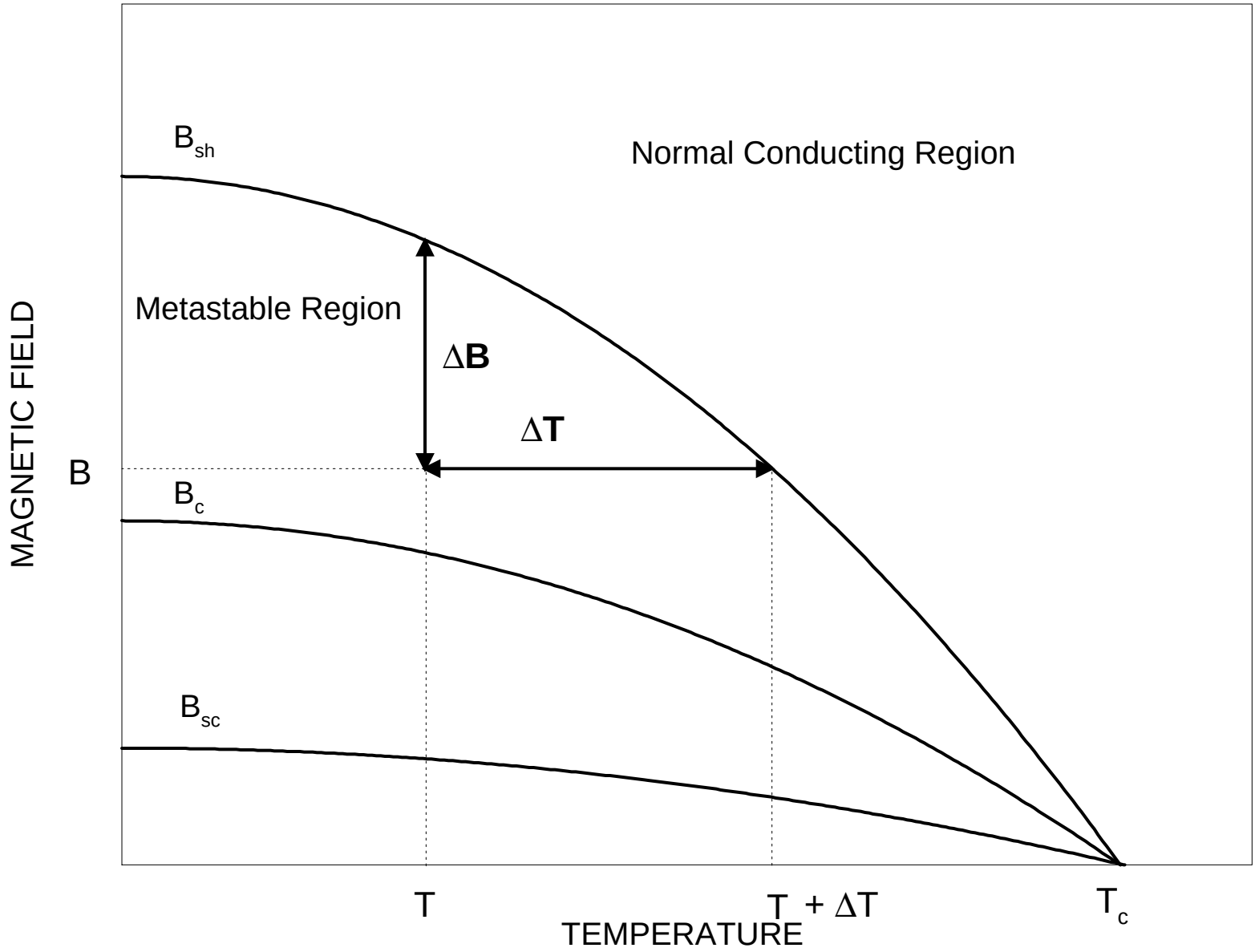

Fig. 2 Penaranda et al.

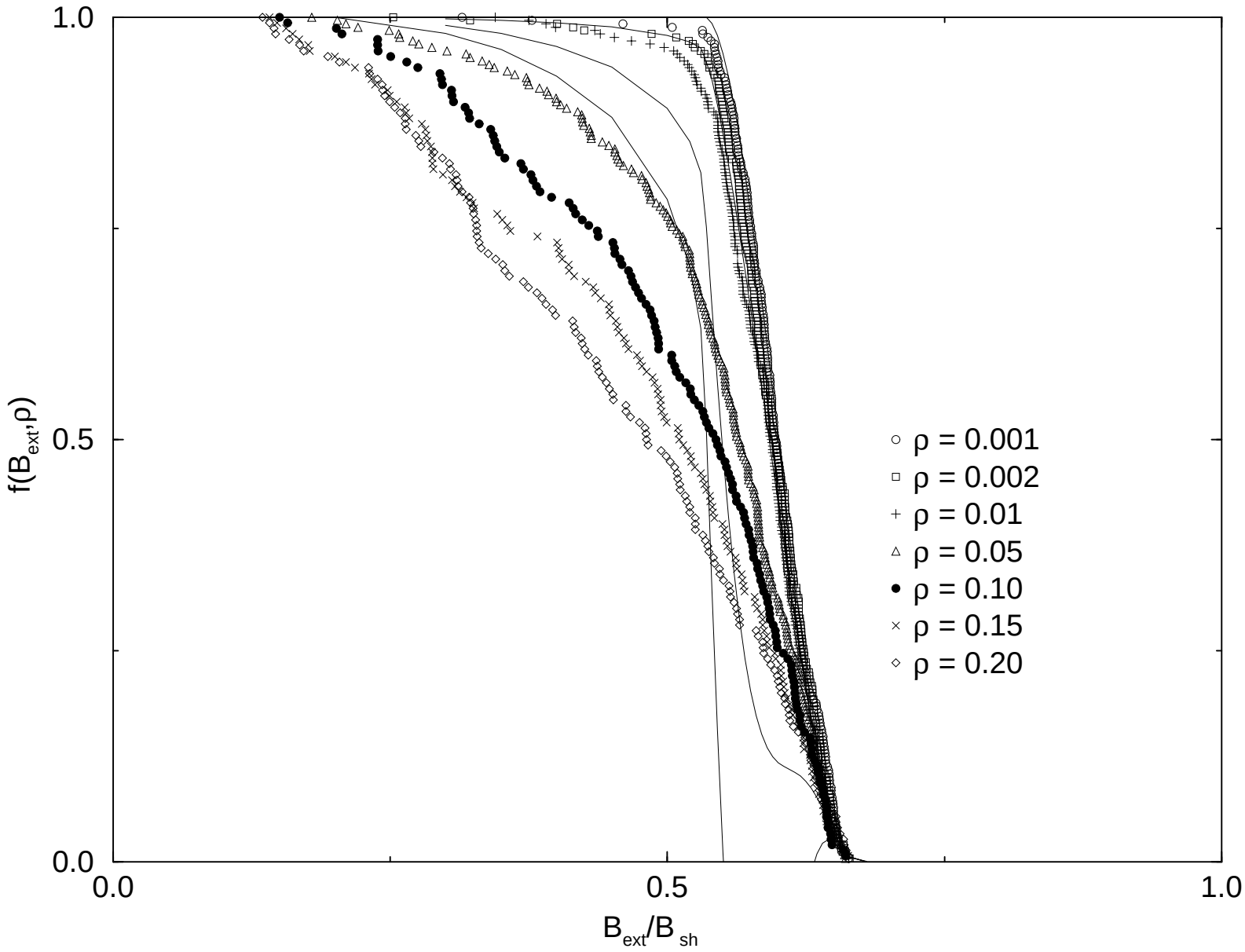

Fig. 3 Penaranda et al.

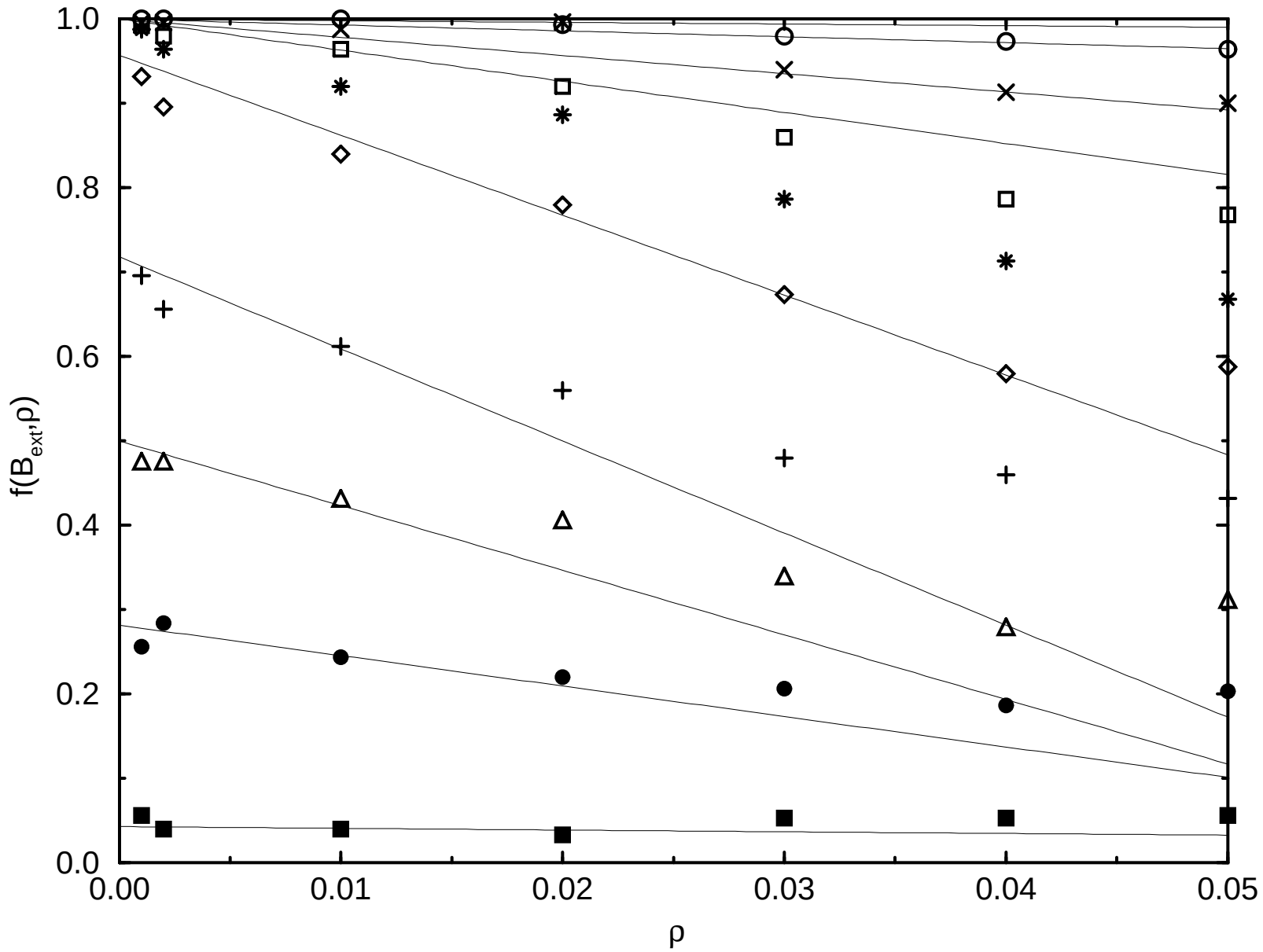

Fig. 4 A. Penaranda et al.

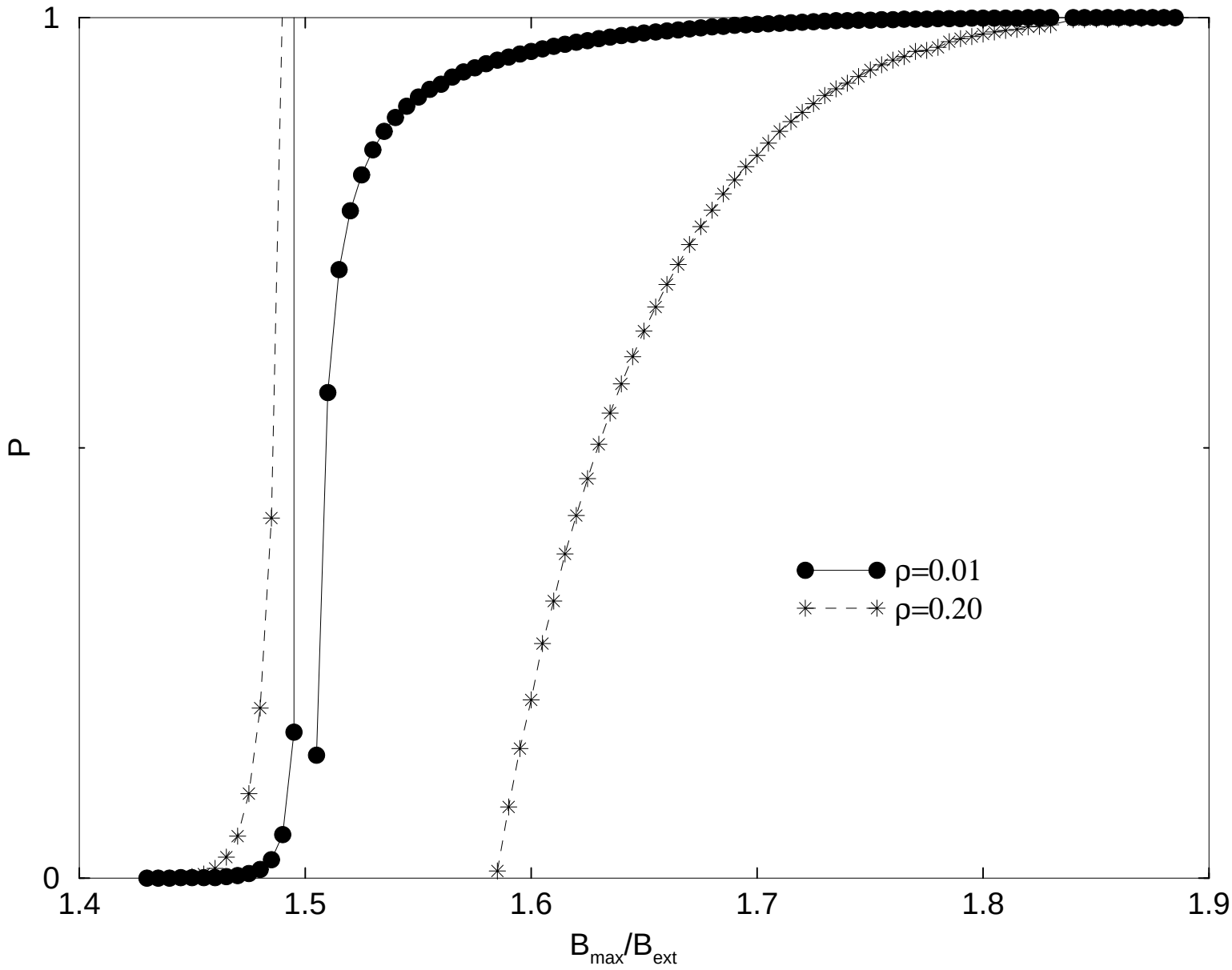

Fig. 5 A. Penaranda et al.

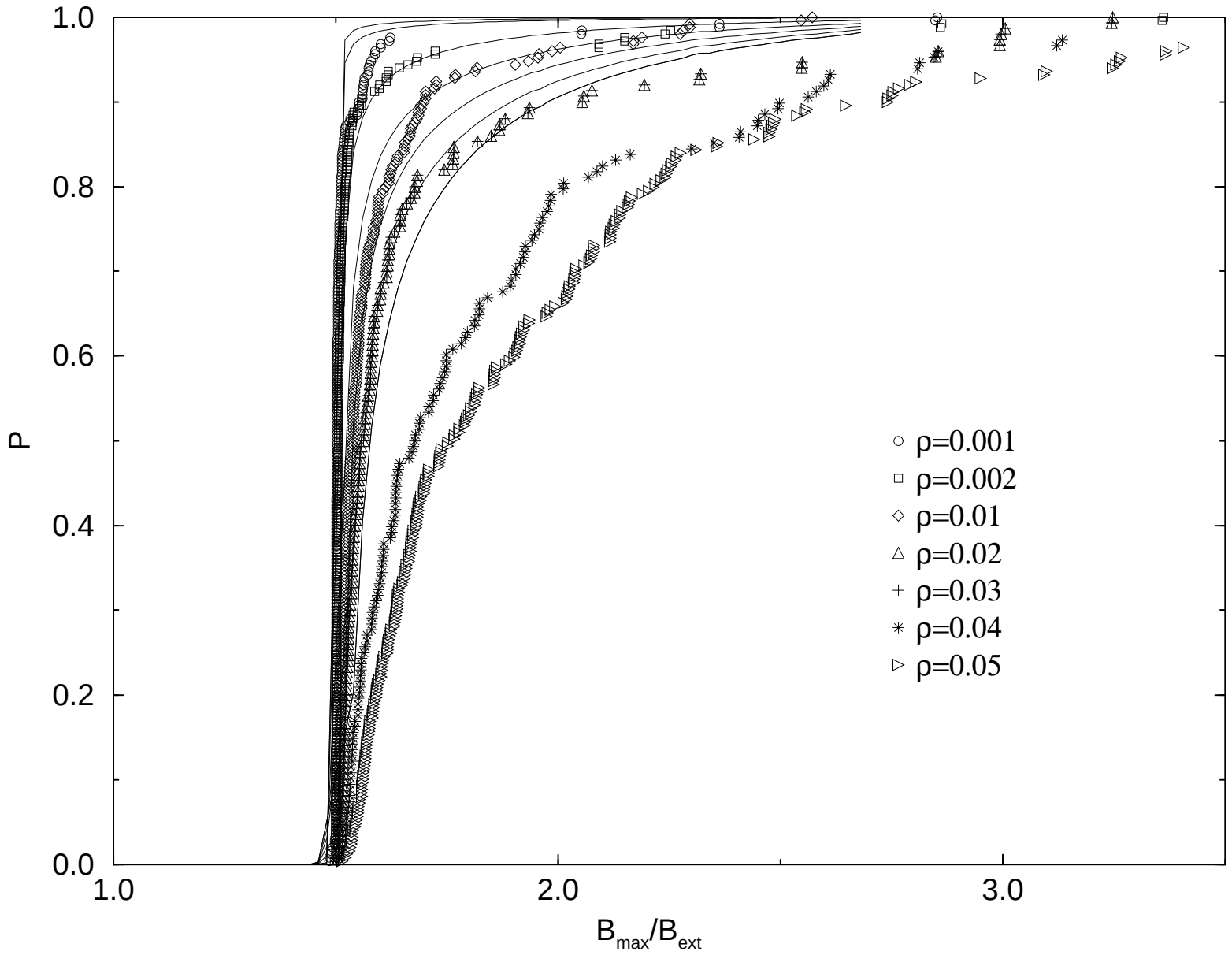

Fig. 6 A. Penaranda et al.

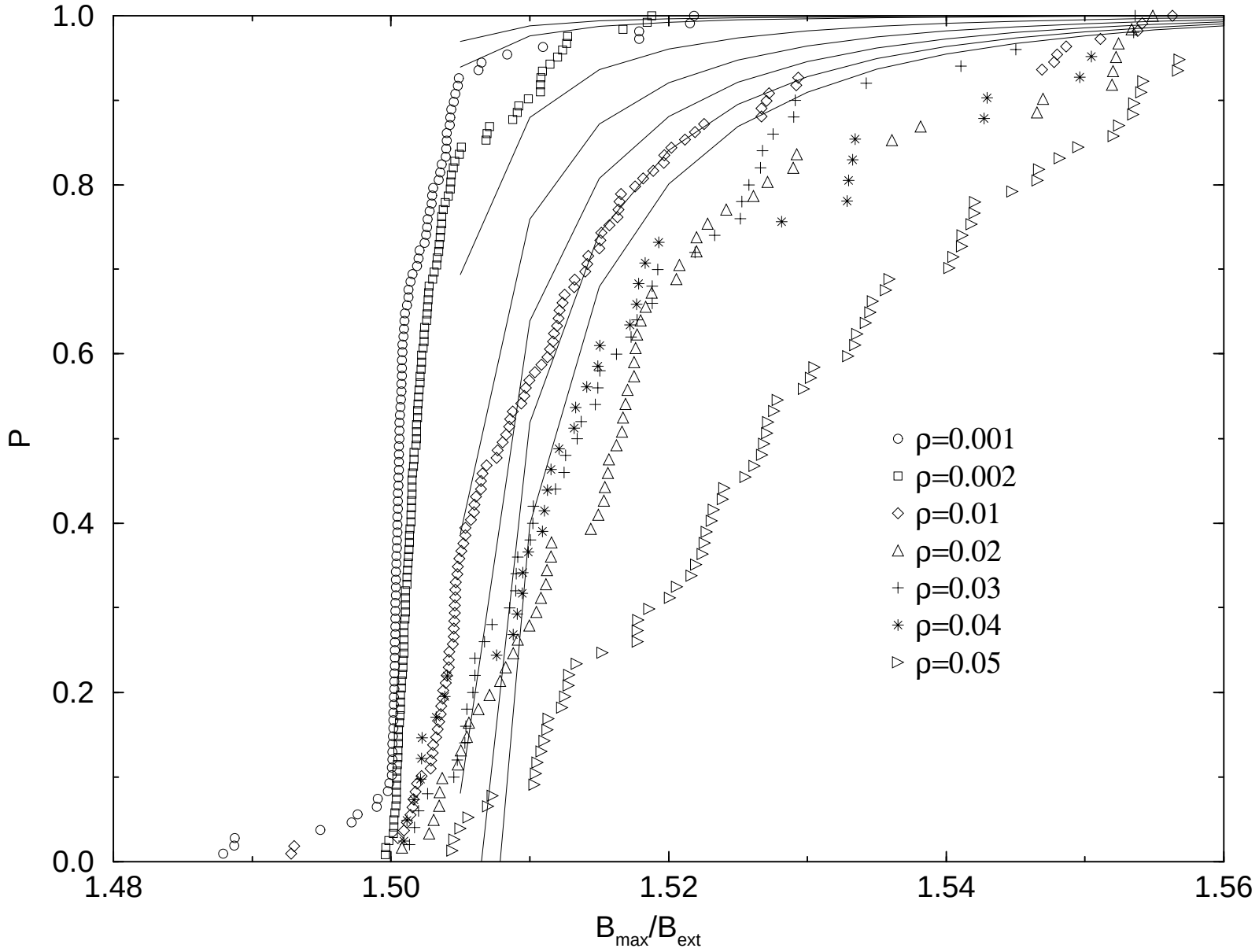

Fig. 7 Penaranda et al.

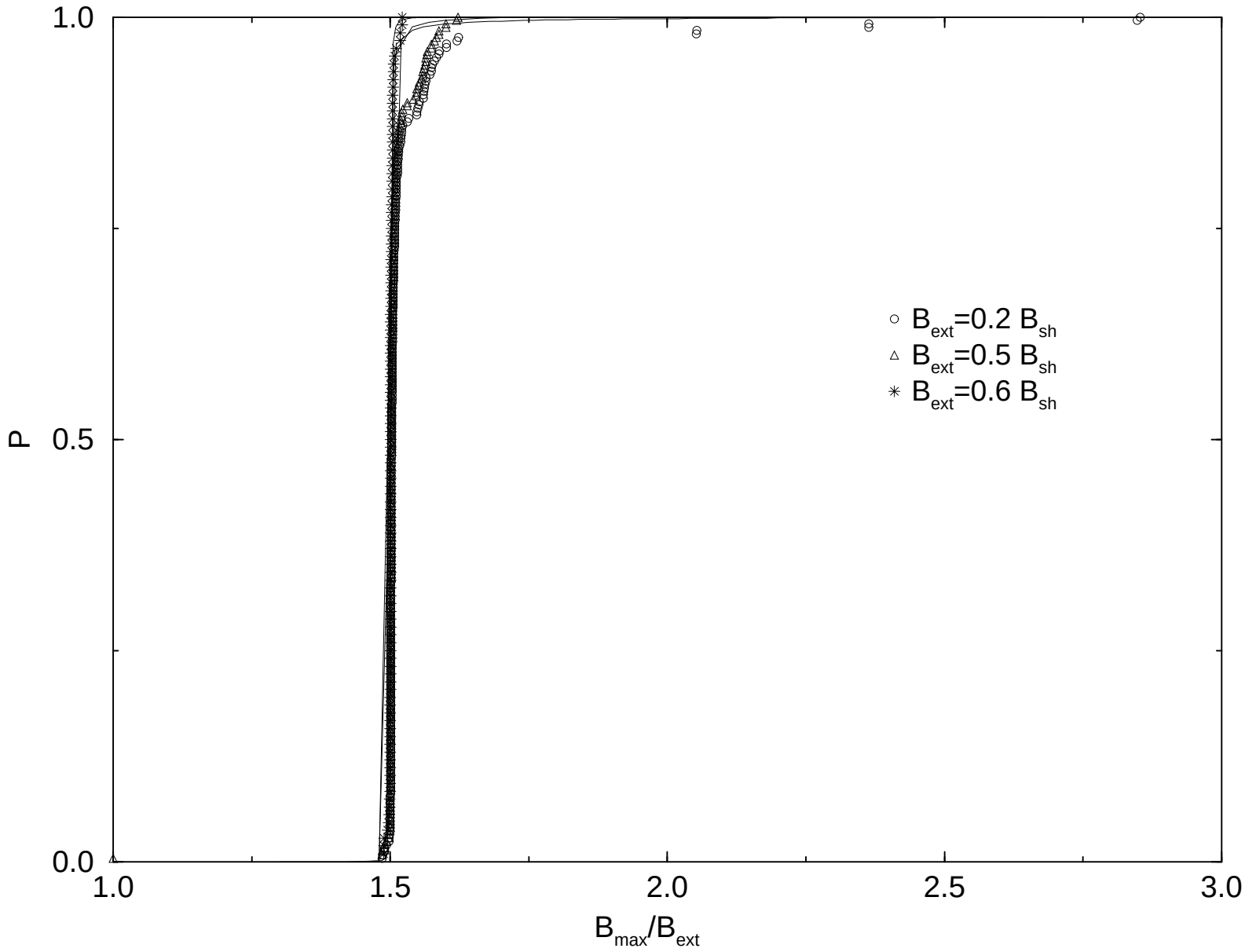

Fig. 8 A. Penaranda et al

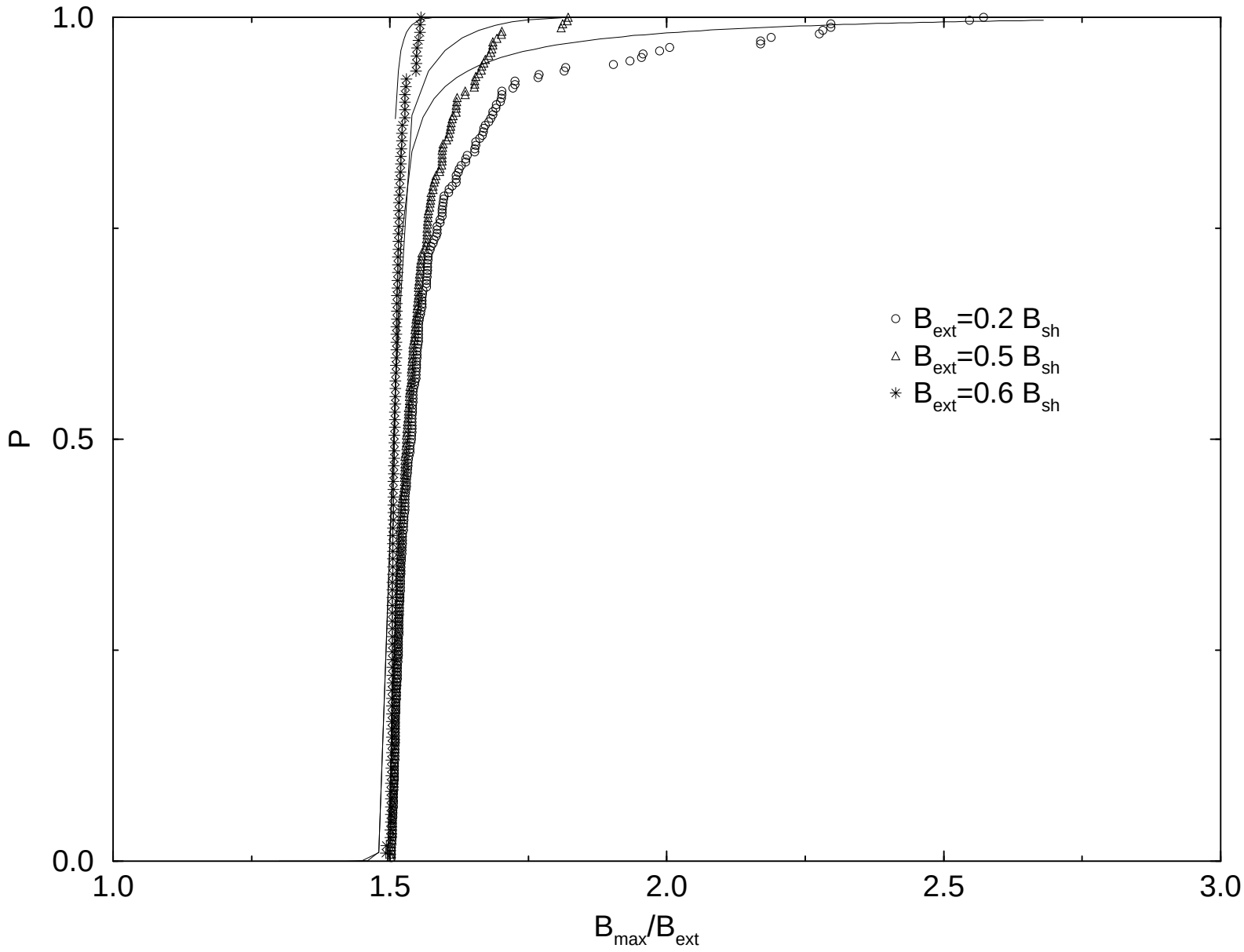

Fig. 9 A.Penaranda et al.

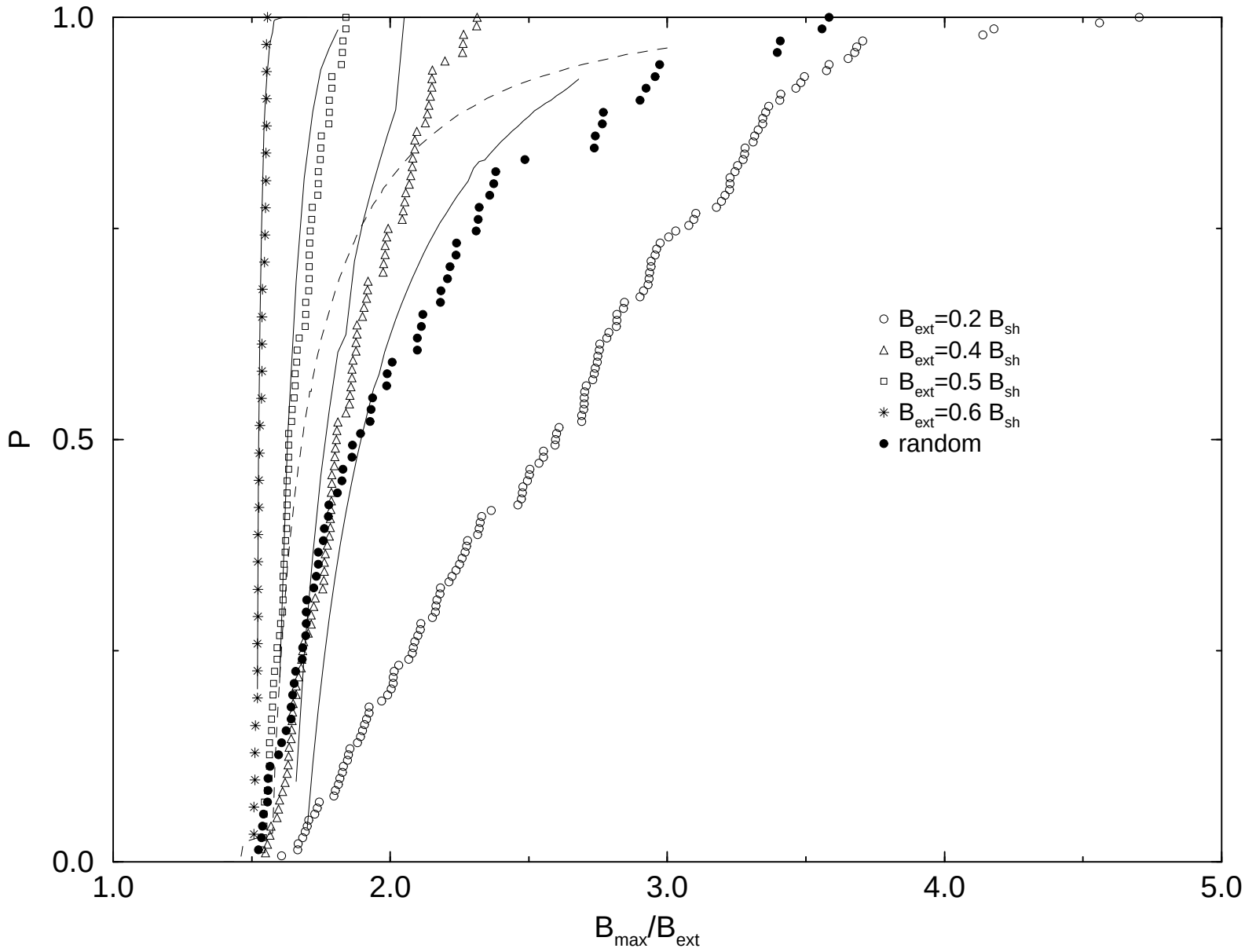

Fig. 10 A. Penaranda et al

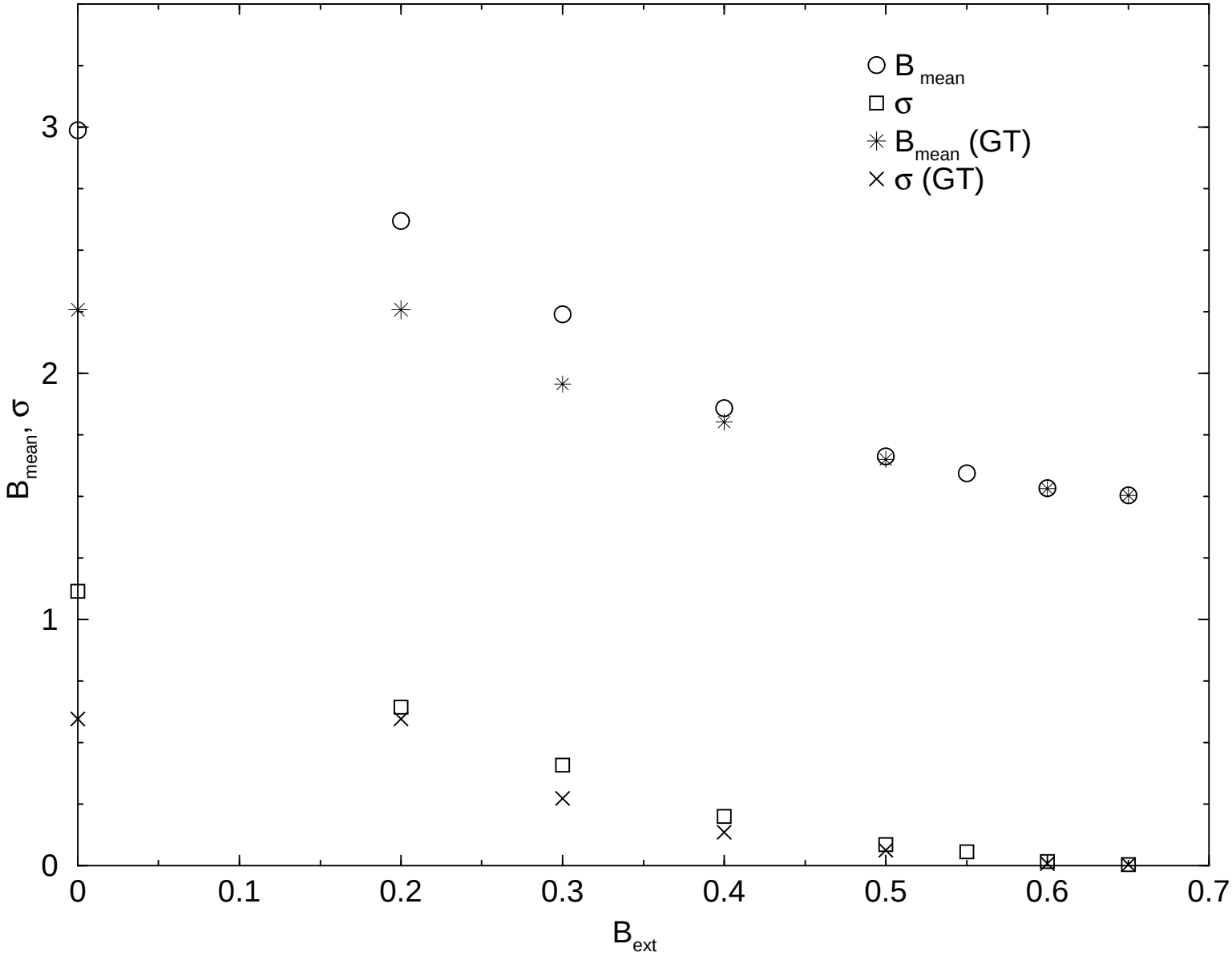

Fig. 11 Penaranda et al